doi:10.1093/brain/awq071 Brain 2010: 133; 1391–1402 | 1391

BRAIN
A JOURNAL OF NEUROLOGY

A mutation affecting the sodium/proton exchanger, *SLC9A6*, causes mental retardation with tau deposition

James Y. Garbern,[1,2] Manuela Neumann,[3,4] John Q. Trojanowski,[4] Virginia M.-Y. Lee,[4] Gerald Feldman,[2,5] Joy W. Norris,[6] Michael J. Friez,[6] Charles E. Schwartz,[6] Roger Stevenson[6] and Anders A. F. Sima[1,5]

1 Department of Neurology, Wayne State University School of Medicine, Detroit 48201, MI, USA
2 Centre for Molecular Medicine and Genetics, Wayne State University School of Medicine, Detroit 48201, MI, USA
3 Institute of Neuropathology, University Hospital of Zürich, Zürich CH-8091, Switzerland
4 Centre for Neurodegenerative Disease Research, Department of Pathology and Laboratory Medicine, and Institute on Aging, University of Pennsylvania School of Medicine, Philadelphia, PA 19104, USA
5 Department of Pathology, Wayne State University School of Medicine, Detroit 48201, MI, USA
6 Greenwood Genetics Centre, Greenwood, SC 29646, USA

Correspondence to: James Y. Garbern,
421 E Canfield,
Room 3217
Detroit,
MI 48201, USA
E-mail: jgarbern@med.wayne.edu

We have studied a family with severe mental retardation characterized by the virtual absence of speech, autism spectrum disorder, epilepsy, late-onset ataxia, weakness and dystonia. Post-mortem examination of two males revealed widespread neuronal loss, with the most striking finding being neuronal and glial tau deposition in a pattern reminiscent of corticobasal degeneration. Electron microscopic examination of isolated tau filaments demonstrated paired helical filaments and ribbon-like structures. Biochemical studies of tau demonstrated a preponderance of 4R tau isoforms. The phenotype was linked to Xq26.3, and further analysis identified an in-frame 9 base pair deletion in the solute carrier family 9, isoform A6 (*SLC9A6* gene), which encodes sodium/hydrogen exchanger-6 localized to endosomal vesicles. Sodium/hydrogen exchanger-6 is thought to participate in the targeting of intracellular vesicles and may be involved in recycling synaptic vesicles. The striking tau deposition in our subjects reveals a probable interaction between sodium/proton exchangers and cytoskeletal elements involved in vesicular transport, and raises the possibility that abnormalities of vesicular targeting may play an important role in more common disorders such as Alzheimer's disease and autism spectrum disorders.

Keywords: mental retardation; corticobasal degeneration; tau expression; *SLC9A6*; autism

Abbreviations: PHF = paired helical filaments; SDS–PAGE = sodium dodecyl sulphate polyacrylamide gel electrophoresis; SLC9A6 = solute carrier family 9, isoform A6; TDP-43 = transactivation response element DNA-binding protein

Received January 21, 2010. Revised February 17, 2010. Accepted February 24, 2010. Advance Access publication April 15, 2010

Introduction

Mental retardation affects an estimated 2–3% of the population. About 25% of mental retardation is believed to be caused by genetic abnormalities, and up to 10% is estimated to be caused by X chromosome mutations, accounting in part for the observed male preponderance of mental retardation (reviewed in Ropers, 2006). While fragile X mental retardation-1 is the most common cause of hereditary mental retardation, many other X chromosome mental retardation loci have been characterized. Over 50 genes have been identified that are associated with syndromic, or clinically distinctive, X-linked mental retardation, and over 15 genes have been found to be associated with non-syndromic, or clinically indistinguishable X-linked mental retardation (http://www.ggc.org/xlmr.htm). Over 100 additional X chromosome loci have been linked to non-syndromic and syndromic mental retardation for which the genes have not yet been identified. Since the candidate chromosomal loci for some of these families overlap, and allelic heterogeneity can occur, it is possible that this number may be an overestimate. The distinction between syndromic and non-syndromic mental retardation is not precise, and conditions previously regarded as non-syndromic forms of mental retardation may have additional clinical findings that were not initially recognized or emphasized, such as the cerebellar hypoplasia seen in mutations of the oligophrenin 1 (*OPHN1*) gene (Philip *et al.*, 2003).

Here, we report a family with a novel, syndromic form of severe X-linked mental retardation with autistic behaviour, seizures and wide-spread neuronal degeneration that is associated with filamentous neuronal and glial deposits of the microtubule-binding protein tau in cortical and sub-cortical regions. Tau-positive inclusions are the defining neuro-pathological characteristics of a number of adult-onset neuro-degenerative disorders (subsumed as tauopathies), including Alzheimer's disease, progressive supranuclear palsy, corticobasal degeneration and Pick disease, as well as familial forms of fronto-temporal dementia (FTDP-17T), which are associated with mutations in the gene that encodes tau, *MAPT* (Sima *et al.*, 1996; Lee *et al.*, 2001). The central nervous system (CNS) tau pathology in two affected members of this family with X-linked mental retardation was analysed using histological, immuno-histochemical, biochemical and ultrastructural methods. Our data demonstrate that solute carrier family 9, isoform A6 (*SLC9A6*)-related mental retardation can be associated with a tauopathy characterized by neuronal and glial tau inclusions. To our knowledge these tau-positive inclusions have not been associated with early-onset mental retardation or autism.

Materials and methods

Clinical

Subjects were evaluated through an Institutional Review Board-approved protocol, and consent for blood testing and autopsy was obtained from the subjects' parents or guardians.

Linkage analysis

Twenty-nine evenly spaced microsatellite markers on the X chromosome were genotyped. The forward primers were synthesized with a fluorescein-tag (Fluore Prime, Amersham) at the 5′-end. Microsatellite polymorphisms were analysed on the CEQ 8800 (Beckman Coulter) using the Fragment manager software. Two-point and multipoint linkage analyses were performed using Perl scripts (available for download at http://bioinfo.ggc.org/ggcepi/linkage.html) that automate the use of the FASTLINK package (Lathrop *et al.*, 1984; Cottingham *et al.*, 1993). The disease gene frequency was set at 0.0001, and full penetrance in males and no penetrance in females were assumed. Once a linked region was observed, the region was further refined by genotyping and analysing additional markers.

Mutation screening

The coding exons and their flanking regions of *SLC9A6* were amplified from genomic DNA and sequenced using an Applied Biosystems 3730 automated DNA Analyser. Sequencing was performed in both directions.

MAPT genetic analysis

Genomic DNA was extracted from frozen brain tissue using a magnetic particle-based system (MagAttract DNA M48 Mini kit; Qiagen, Chatsworth, CA, USA) on an automated platform (BioRobot M48; Qiagen) according to the manufacturer's protocol. Exons 1, 9–13 of the *MAPT* gene were amplified for direct DNA sequencing using primers corresponding to flanking intronic sequences.

Pathological analysis

The brains from two cases, III-9 and III-11, were examined pathologically. At the time of autopsy, the brains were weighed and samples were obtained from various regions and snap-frozen in liquid nitrogen. The brains were then suspended in 10% buffered formalin for at least 2 weeks. At brain cutting, the gross aspects of the brain were recorded. Routine histological analysis was performed on paraffin-embedded material and stained with haematoxylin–eosin, luxol fast blue, Bielchowsky's silver stain and Congo red according to standard clinical protocols.

Immunohistochemistry

Formalin-fixed tissue samples were paraffin embedded, and cut into 6 μm thick sections. Immuno-histochemistry was performed as previously described using the ABC method (Vectastatin ABC kit, Vector Laboratories, Burlingame, CA, USA) and 3,3′-diaminobenzidine (Schmidt *et al.*, 1987; Mawal-Dewan *et al.*, 1996; Forman *et al.*, 2002). The following primary antibodies were used: anti-human neurofilament-L monoclonal mouse antibody, clone 2F11 (1:100; Dako AS, Glostrup, Denmark), anti-tau monoclonal mouse antibodies paired helical filament (PHF)-1 (1:1000, gift from P. Davies, Albert Einstein College of Medicine, Bronx, NY, USA) (Greenberg and Davies, 1990) and AT-8 (1:1000) (Mercken *et al.*, 1992; Goedert *et al.*, 1995), affinity-purified polyclonal anti-tau antibody 17025 (1:3000) (Zhukareva *et al.*, 2002), anti-α-synuclein monoclonal mouse antibody LB509 (1:1000) (Giasson *et al.*, 2000) and anti-transactivation response element DNA binding protein (TDP-43) polyclonal antibody (1:1000; ProteinTech Group, Chicago, IL, USA). The sections were viewed with a Nikon FXA microscope and images were captured with the RS Image software (Roper Scientific Inc.,

Duluth, GA, USA). For semi-quantitative assessments of the different pathological abnormalities, the scoring was defined as: 0 = none, 1 = mild, 2 = moderate and 3 = severe.

Biochemical and western blot analysis

Frozen tissue samples for biochemical analysis were available from frontal and occipital cortices of Case III-9 and frontal cortex, basal ganglia and cerebellum of Case III-11.

Phosphorylated and dephosphorylated sarkosyl-insoluble samples were prepared as previously described (Lee *et al.*, 1991; Hong *et al.*, 1998; Winton *et al.*, 2006). The solubility profile of tau was analysed on sequential extractions of brain samples using methods reported earlier (Forman *et al.*, 2002). For western blot analysis, protein extracts were resolved by 7.5% sodium dodecyl sulphate polyacrylamide gel electrophoresis (SDS–PAGE) and transferred to nitrocellulose membranes and probed with a mixture of anti-tau monoclonal antibodies T14 (1:3000) (Kosik *et al.*, 1988; Hong *et al.*, 1998) and T46 (1:1000) (Kosik *et al.*, 1988; Hong *et al.*, 1998) as well as phosphorylation-dependent anti-tau monoclonal antibodies AT8 (Goedert *et al.*, 1993) (1:500, Innogenetics, Ghent, Belgium), PHF-1 (Greenberg and Davies, 1990) (1:500, gift from Dr P. Davies, Albert Einstein College of Medicine, Bronx, NY, USA) and 12E8 (Seubert *et al.*, 1995) (1:1000, gift from Dr P. Seubert, Elan Pharmaceuticals, South San Francisco, CA, USA). Six recombinant human brain tau isoforms were used as a standard for the western blot studies. Monoclonal antibodies were detected with horseradish peroxidase-conjugated anti-mouse immunoglobulin G (Santa Cruz Biotechnologies, Santa Cruz, CA, USA) and signals were revealed by a horseradish peroxidase-based chemiluminescent reaction (Pierce, Rockford, IL, USA).

Electron microscopy of isolated filaments

Dispersed tau filaments were prepared from separately dissected cortical grey and white matter, adsorbed on carbon-coated 400-mesh grids, and stained with 0.4% uranyl acetate as described (Zhukareva *et al.*, 2002). Grids were examined with a JEM1010 electron microscope at 80 kV.

Results

Clinical description of the family

The pedigree of this family is shown in Fig. 1. The family is of mixed, non-consanguineous English, Welsh and Scottish descent. At least six males had severe mental retardation that was apparent during early childhood, with little to no language acquisition, but relatively preserved gross motor development. The affected males displayed little interest in social interaction and did not play with family or schoolmates. They displayed little emotional response and remained aloof. The affected individuals were graded as severely autistic using the Childhood Autism Rating Scale (Schopler *et al.*, 1980). Several of the affected males had stereotyped, repetitive hand movements, reminiscent of patients with Rett syndrome. Progressive motor deterioration and ataxia were observed in the affected males beginning in the fourth to fifth decade of life. In two of the affected males, unilateral weakness and spasticity developed prior to the loss of ambulation. The MRI of Patient III-9 did not show cerebellar atrophy of significant structural anomalies, except for an incidental cavernous haemangioma and moderate atrophy (Fig. 2).

Linkage analysis

Linkage mapping using 29 microsatellite markers on the X chromosome localized the disease locus in family K9071 between markers DXS1047 (Xq26.1) and DXS8106 (Xq27.1), an interval of 13.1 Mb (Supplementary Table 1). A maximum LOD score of 2.0 was obtained for DXS994, DXS8041, DXS1192 and DXS984. Multipoint analysis yielded a maximum LOD score of 2.4 (Supplementary Fig. 1) and the disease locus was tightly linked between markers DXS984 and DXS994, an interval of 9.3 Mb. One hundred and seventeen genes have been identified in this area. Among these are genes already known to be involved in X-linked mental retardation, such as *GPC3, PHF6, ARJGEF6, FGF13, SLC9A6, αPIX, ZDHHC9, HPRT, OCRL1* and *SOX3*. Other candidate genes from the area include two genes that

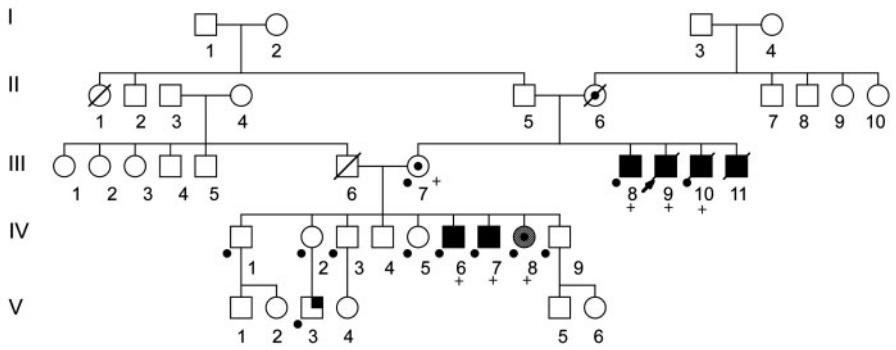

Figure 1 Pedigree of the family. Patient IV-8 is mildly retarded but has acquired good language skills. Patient V-3, by age 5 years, had acquired some receptive language ability, was able to operate a videotape player and other household appliances and had been diagnosed as mildly autistic, and is highlighted by the corner square. The propositus is indicated by an arrow. The subjects who were examined and from whom DNA samples were obtained are indicated by a dot to the lower left of the individual's icon. Plus symbols indicate individuals who have the c.1012_1020del mutation in *SLC9A6*. Female heterozygotes are indicated by the central dot.

encode the zinc finger proteins, ZNF75 and ZNF449, and two genes that are expressed in the brain, *MST4* and *GPC4*.

Recently, *SLC9A6* mutations have been shown to cause a severe syndromic form of X-linked mental retardation, in a family originally described by Christianson *et al.* (1999). The phenotypic similarity of affected males in this family to that described by Christianson *et al.* and the linkage to Xq26.3 led to analysis of *SLC9A6*. Sequencing of the coding sequence of *SLC9A6* using genomic DNA from one affected male in the family detected a 9 base pair deletion, c.1012_1020del (Refseq NM_006359.2) in exon 8. Sequence analysis of other members of the family found this 9 base pair deletion segregated with the X-linked mental retardation phenotype (Fig. 1). The 9 base pair deletion results in an in-frame deletion of three amino acids, p.Trp338_Thr340del (p.Trp392_Thr394del of the longer transcript refseq NM_001042537). These amino acids fall within a domain, conserved at least through zebrafish, of *SLC9A6* and that abuts a potential transmembrane domain from amino acid residues 340–360 (394–414).

The clinical findings for all six affected males are summarized in Table 1 and compared to the clinical findings described by Christianson *et al.* (1999) and Gilfillan *et al.* (2008), who described three additional families in addition to those originally described by Christianson *et al.* (1999). An Angelman-like phenotype was not observed in any of the affected males. Although head circumference was below average, microcephaly was not as prominent as observed in the families described by Gilfillan *et al.* (2008), whose head circumferences were 2–4 cm, below the 2.5 percentile.

Neuropathological examination

Two members of the family died and, with the family's informed consent, post-mortem analysis was conducted. The findings were similar in the specimens from Patients III-9 and III-11, except for a left occipital cavernous haemangioma, judged to be a coincidental finding, in Patient III-9. There was generalized and symmetric cerebral atrophy, with brain weights of 1020 and 950 g, respectively. Both specimens had generalized atrophy of the white matter and moderate dilatation of the ventricles. The cortex was unremarkable and well demarcated. The head of the caudate, putamen and globus pallidus appeared small and discoloured. Cerebellum was moderately atrophied. There was pallor of the substantia nigra and locus coeruleus. The spinal cords were unremarkable. The most striking histological findings were marked neuronal loss and gliosis of the globus pallidus, putamen, substantia nigra and cerebellar cortex (Fig. 3A and Table 2). Less severe neuronal loss and gliosis were seen in the caudate nucleus, pontine and inferior olivary nuclei and in the cerebellar dentate nucleus (Table 2). The cerebral cortex and hippocampus were only mildly involved (Table 2). The centrum semiovale, cerebellar and brainstem

Table 1 Clinical features of SLC9A6-related mental retardation

CNS features	III-8 53 years	III-9 49 years	III-10 47 years	III-11	IV-4 23 years	IV-5[a] 22 years	%	Christianson syndrome	Gilfillan *et al.* (families 1–3)
Profound mental retardation	+	+	+	+	+	+	100	16/16 (100)	3/3
Autistic behaviour	+	+	+	+	+	+	100	2/4 (50)[b]	
Microcephaly[c]	−(55.9)	−(54)	+(53)	+(53.3)	−(55.5)	−(54)	33	3/4 (75)	3/3
Mutism	+	−	+	+	+	−	66.7	16/16 (100)	3/3
Incontinence	+	+	+	+	+	+	100	14/14 (100)	
Epilepsy	+	−	+	+	+	+	83.3	14/14 (100)	3/3
Ophthalmoplegia	+	+	+	+	−	+	83.3	3/3 (100)	3/3
Truncal ataxia	+	+	+	+	+	+	100	3/3 (100)	
Non-ambulatory	−	−	−	−	−	−	0	7/16 (43.75)	
Late ambulation	+	−	+	+	−	+	66.7	9/16 (56.25)	
Adducted thumbs	−	−	−	−	−	−	0	5/8 (62.5)	
Dystonia	+	+	+		+	+	83.3		
Maladaptive behaviour	+	+	+	+	−	−	66.7		
Hand-wringing	+	+	+	+	−	−	66.7		
Hemiparesis	−	+	+	−	−	−	33.3		
Angelman-like syndrome	−	−	−	−	−	−	0	0	3/3
Craniofacial features									
Long, narrow face	−	−	−	−	−	+[a]	16.7	5/5 (100)	1/3
Large ears	−	−	−	−	−	−	0	7/7 (100)	
Square, prognathic jaw	−	−	−	−	−	+[a]	16.7	5/5 (100)	
Long, aquiline nose	−	−	−	−	−	+[a]	16.7	5/5 (100)	

Clinical features of the family; percentage of family members with the clinical sign is given in column 8. For comparison, the numbers and percentages (in parentheses) of family members described by Christianson *et al.* (1999) and by Gilfillan *et al.* (2008), are presented in the following two columns. Patient III-11 is deceased and had not been examined by any of the authors. His clinical findings were obtained from his medical records and examination of photographs.

a Patient also has a chromosomal translocation: 46, XY, *t*(14;18)(q13;q23).

b Based on the detailed narrative descriptions of four patients.

c Figures in parentheses are occipito-frontal head circumferences (cm). Microcephaly was present if the height-adjusted head circumference was less than the 3rd percentile for adults, as defined by Bushby *et al.* (1992).

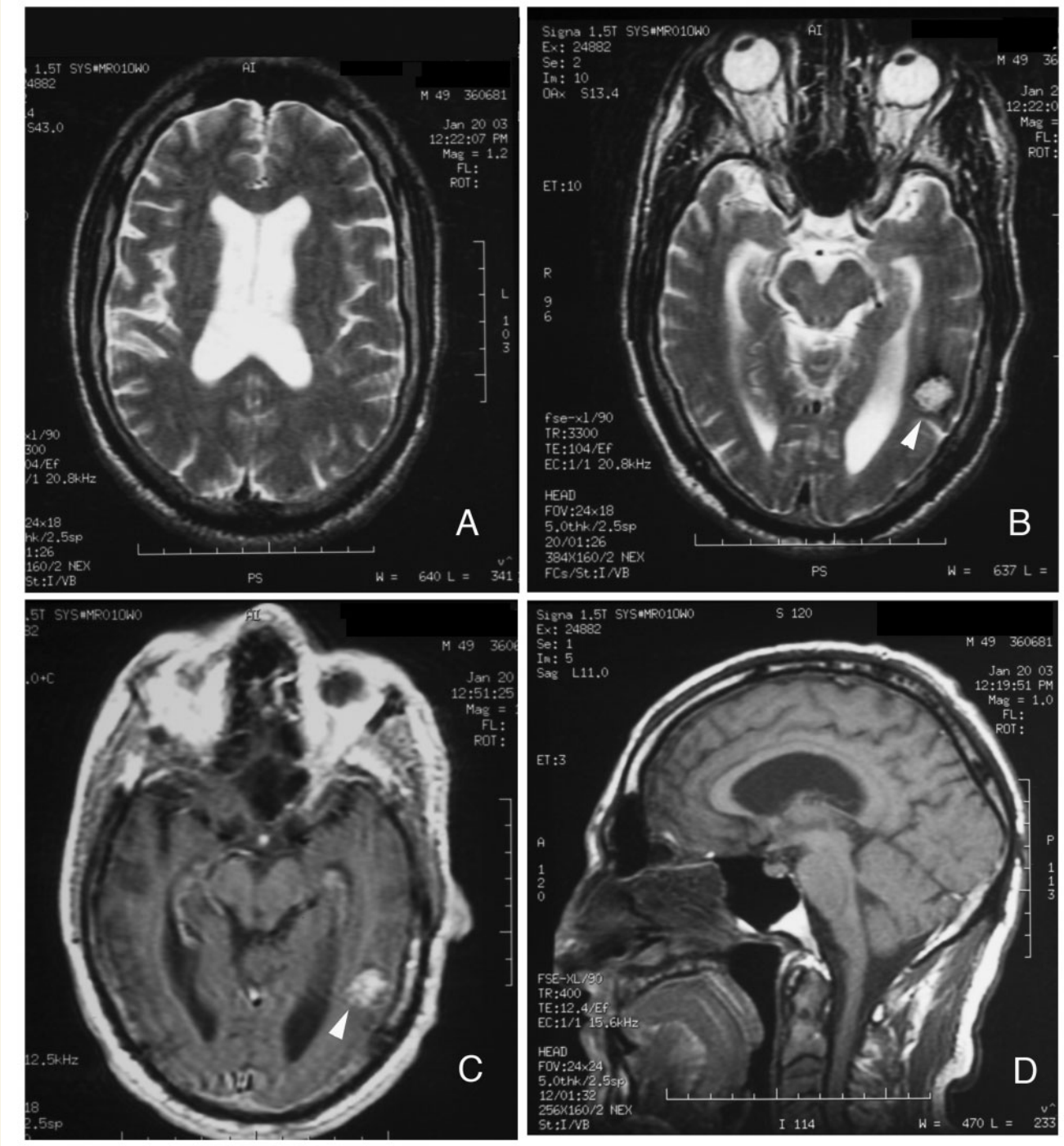

Figure 2 Representative MRI slices from Patient III-9. (**A**) Axial T_2-weighted image showing moderate ventricular enlargement and sulcal widening with normal appearance of white matter. (**B**) Axial T_2-weighted image at level of midbrain. In addition to the atrophied appearance of the brain, there is a left parieto-occipital lesion (arrowhead) with evidence of surrounding past haemorrhage (dark rim). (**C**) Gadolinium enhanced T_1-weighted slice showing enhancement of the left parieto-occipital lesion (arrowhead). (**D**) T_1 sagittal slice through the midline showing thin corpus callosum and moderate sulcal prominence and ventricular dilatation.

white matter tracts showed diffuse glial tau pathology. The spinal cord was unremarkable except for occasional dystrophic axons in the anterior and dorsal horns.

Numerous tau-positive inclusions resembling coiled bodies were seen in glial cells throughout the white matter (Fig. 3B). A striking finding was widespread, strongly tau-positive tangle-like inclusions, commonly seen in neurons in the substantia nigra (Fig. 3C), locus coeruleus, pontine nuclei, basal ganglia, thalami and cranial nerve nuclei (Fig. 3D and Table 2). These were also seen in the cerebral cortex and hippocampus (Table 2). Tau-positive astrocytic plaques were seen in the cerebral white matter, thalamus and brainstem (Fig. 3E). Tau-positive inclusions

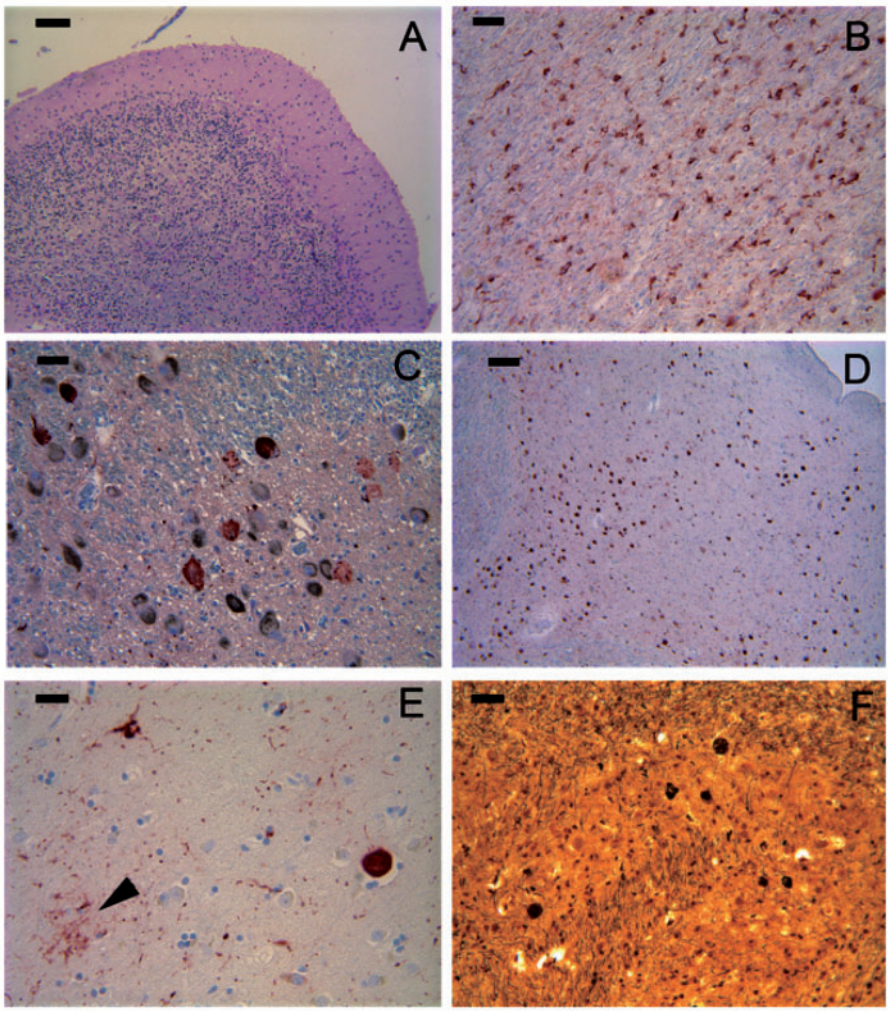

Figure 3 Histological and immunohistochemical analyses. (**A**) Cerebellar cortex from Patient III-9 showing severe loss of Purkinje cells and neuronal loss in the internal granular layer. Haematoxylin–eosin stain, scale bar = 300 μm. (**B**) Cerebral white matter from Patient III-11 stained with anti-tau showing diffuse abundant positive staining of white matter glial elements. Scale bar = 100 μm. (**C**) Tau-stained substantia nigra from Patient III-9 showing frequent tau-positive neuronal inclusions. Scale bar = 20 μm. (**D**) Tau immunostaining of the third cranial nerve nucleus from Patient III-11 shows abundant positive staining of the neuronal population. Scale bar = 200 μm. (**E**) Tau-positive astrocytic plaque (arrowhead) in the dorsal raphae nucleus in Patient III-9. Scale bar = 20 μm. (**F**) Bielschowsky silver stain of the dentate nucleus of the cerebellum in Patient III-11 showing frequent silver-positive neuronal inclusions. Scale bar = 50 μm.

stained almost equally well with Bielschowsky's silver stain (Fig. 3F). Neuronal inclusions stained less well for phosphorylated neurofilaments. No α-synuclein or TDP-43 positive inclusions, ballooned neurons or amyloid deposits were identified. The pathological findings are summarized in Table 2.

Biochemical and ultrastructural analyses of tau

To assess the tau isoform composition, sarcosyl-insoluble tau was extracted from affected cortical and sub-cortical brain regions of Patients III-9 and III-11. Immunoblotting with phosphorylation-independent anti-tau monoclonal antibodies, resolved sarkosyl-insoluble tau into two major bands of ~64 and 69 kD and a weaker band of ~60 kD (Fig. 4A). In dephosphorylated samples, tau isoforms comprised a mixture of 3R and 4R isoforms. However, a clear preponderance of 4R isoforms (4R0N and 4R1N) was evident in extracts from affected cortical and sub-cortical brain regions in both cases (Fig. 4A). While the 4R to 3R isoform ratio in Alzheimer's disease and control brains is ~1 (Hong *et al.*, 1998; Zhukareva *et al.*, 2002), quantitative analysis of the band intensities revealed an increase of the 4R to 3R ratio up to 2.4 (frontal grey) and 2.2 (frontal white) in Cases III-9 and 2.4 (basal ganglia) in Case III-11.

Ultrastructural analysis of the tau filaments in the sarkosyl-insoluble material revealed a mixture of PHF-like structures (maximum width 15–20 nm, distance between crossovers 70–80 nm) and ribbon-like structures (maximum width 17–22 nm, distance between crossovers 150–240 nm; Fig. 4B).

To characterize pathological tau proteins further in these cases, we conducted studies of a wide spectrum of tau proteins ranging from soluble to very insoluble species using a graded sequential

Table 2 Severity of neuronal loss and gliosis and frequencies of tau-positive and Bielchowsky-positive neuronal and glial inclusions as well as phosphorylated neurofilament inclusions

	Neuronal loss	Glial fibrillary acidic protein	Bielschowsky		Tau		Neurofilament
			Neurons	Glia	Neurons	Glia	
Cortex							
Frontal	0.5	1.0	1.5	1.0	1.5	1.5	1.0
Entorhinal	1.0	1.5	2.0	1.0	2.0	0.5	1.0
Parietal	0	0.5	1.5	1.0	1.0	0.5	1.0
Occipital	0.5	0.5	1.0	0.5	1.0	2.0	1.5
Hippocampus							
CA_1	1.0	2.0	1.0	0.5	1.5	0.5	0.5
CA_2	0.5	1.0	0.5	0.5	1.0	0.5	0.5
CA_3	0	0.5	0.5	0.5	1.5	0.5	0.5
CA_4	0.5	2.0	0.5	0.5	0.5	0.5	1.0
Subiculum	0.5	2.0	2.0	1.0	2.0	0.5	1.0
Basal ganglia							
Putamen	2.0	1.5	2.0	2.0	2.0	1.0	0.5
Caudate	1.0	2.0	2.0	1.0	2.0	2.0	1.0
Globus pallidus	2.5	2.0	2.0	1.0	2.0	1.5	2.0
Thalamus							
Lateral	0.5	1.5	1.0	1.0	2.0	3.0[a]	0.5
Dorsomedial	1.0	1.5	1.5	1.0	0.5	1.5[a]	0.5
Brainstem							
Substantia nigra	2.5	2.5	2.5	1.5	3.0	2.0	2.0
Third nucleus	1.0	2.0	2.0	0.5	1.5	2.0	0
Fourth nucleus	0.5	1.0	1.5	0.5	1.5	1.5	0
Locus ceruleus	1.5	2.0	2.0	1.0	2.5	2.0[a]	0.5
Fifth nucleus	1.5	1.5	2.5	2.5	1.5	1.5	1.0
Pontine nuclei	1.0	1.5	1.0	0.5	1.5	1.5[a]	0.5
Olivary nucleus	1.0	0.5	1.5	1.5	0.5	2.0	1.5
Cerebellum							
Cortex	2.5	3.0	0	0	0	0	0
Dentate	2.0	2.0	1.5	1.5	2.0	2.0[a]	0.5

The numbers represent severity: 0 = none; 1 = mild; 2 = moderate; 3 = severe. Each number represents the mean of Cases III-9 and III-11.
a Represents presence of tau-positive glial plaques.

series of buffers containing detergents or acids with an increasing ability to solubilize proteins. Highly insoluble tau species as recovered by extraction with 2% SDS buffers were detected in affected cortical regions in Cases III-9 and III-11 revealing a double band of ~64 and 69 kD as well as a high molecular mass smear (Fig. 5A). Western blot analysis with phosphorylation-dependent monoclonal antibodies PHF-1, AT8 and 12E8 showed robust labelling of the 64 and 68 kD bands, and the high molecular mass smear demonstrated that insoluble tau in the studied cases was highly phosphorylated (Fig. 5B).

Molecular genetic analyses

Chromosome analysis of Patient IV-5 revealed an apparently balanced translocation: 46, XY, *t*(14;18)(q13;q23); however, this was not present in his mother, or in Patients III-9 or IV-4. Mutations in the *MECP2* gene, including deletion and duplication of the entire gene, were excluded as was expansion of the Fragile X mental retardation trinucleotide repeat region. To exclude the possibility that the tauopathy in this family is due to a mutation in the tau gene, all exons of the *MAPT* gene in which mutations have been described in familial forms of fronto-temporal dementia so far were sequenced. No mutation was found in the two studied family members described here.

Discussion

The present study describes a novel family with syndromic X-linked mental retardation and autism associated with tau pathology in neurons and glial cells. Clinically, the affected males had severe mental retardation and autistic behaviour, but relative sparing of gross motor abilities (Table 1). Additional clinical signs found in most of the affected males included seizures and late, progressive ataxia that began in the fourth decade. We attribute the dysmorphic features in Patient IV-5 to a chromosomal rearrangement that was not present in the other affected relatives, and which we believe was an independent and unrelated anomaly,

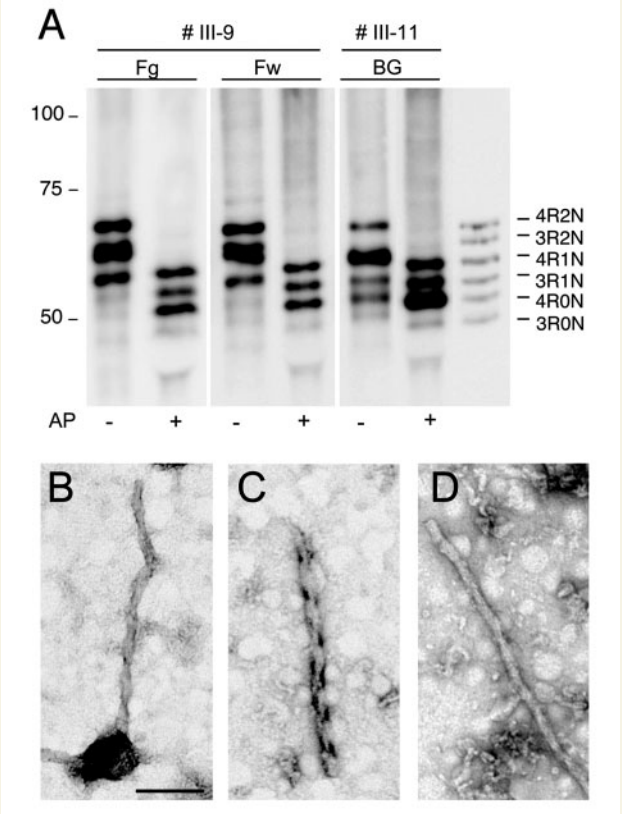

Figure 4 (**A**) Isoform composition of sarkosyl-insoluble tau. Frozen tissue from frontal grey (Fg) and white (Fw) matter and basal ganglia (BG) from Case III-9 were used to extract sarkosyl-insoluble tau species. A portion of each sample was dephosphorylated by incubation with alkaline phosphatase (AP). The dephosphorylated (AP+) and non-dephosphorylated (AP−) samples plus a mixture of six recombinant human brain tau isoforms were resolved on 7.5% SDS–PAGE and immunoblotted with a mixture of monoclonal antibodies T14 and T46. (**B–D**) Ultrastructural analysis of isolated tau filaments revealing paired-helical filament-like structures (**B** and **C**) as well as ribbon-like structures (**D**).

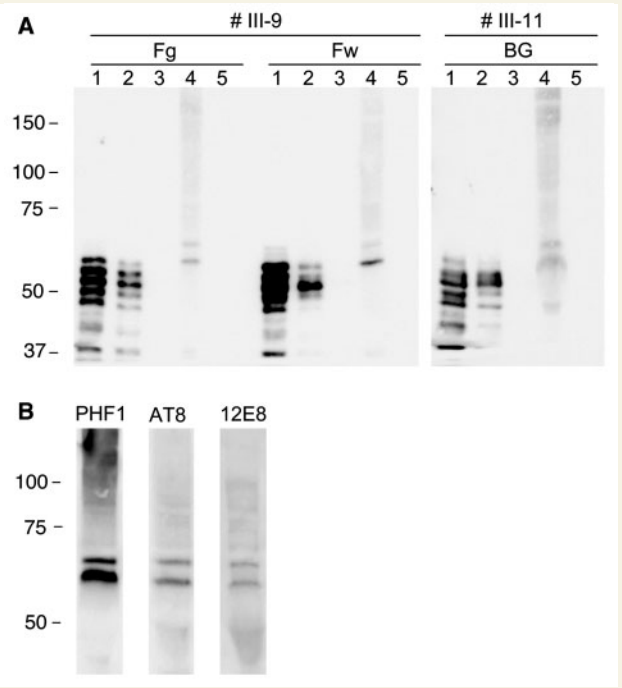

Figure 5 (**A**) Solubility profile of tau proteins. Frontal grey (Fg) and white (Fw) matter from Case III-9 as well as basal ganglia (BG) from Case III-11 were used for sequential extraction of tau with buffers of increasing stringency. Proteins in each fraction were separated by SDS–PAGE and immublotted with a mixture of monoclonal antibodies T14 and T46. 1 = high-salt; 2 = 1% Triton-X100; 3 = radioimmunoprecipitation assay buffer; 4 = 2% SDS; 5 = 70% formic acid fractions. (**B**) Insoluble tau proteins in the 2% SDS fractions are hyperphosphorylated as shown by immunoblotting with phosphorylation-specific monoclonal antibodies PHF1, AT8 and 12E8.

as we also believe was the finding of a cavernous haemangioma in Patient III-9. Since all but one patient had a seizure disorder, and all of the older patients had late onset (after the fourth decade) clinical deterioration, we consider this to be a syndromic form of X-linked mental retardation. The learning disorder present in IV-6 may be caused by unfavourably skewed X-inactivation, dominant inheritance with low penetrance in heterozygous females, variable expressivity or other genetic and non-genetic factors.

We found the family's disorder was caused by a mutation in *SLC9A6*. The syndrome shared profound mental retardation with severe language disturbance with the families described by Christianson *et al*. (1999) and Gilfillan *et al*. (2008). However, the mild dysmorphic features described by Christianson and an Angelman-like syndrome were not observed in the family reported here. Microcephaly was observed in two of the subjects, and does not appear to be as striking as that observed in the patients described by Gilfillan *et al*. (2008). One patient (IV-5) with dysmorphic features also had a coincidental chromosomal translocation not present in other affected family members. The affected males in the family did not play or interact significantly with family members or schoolmates as children or adults. An autistic phenotype was also described in two of the subjects described by Christianson *et al*. (1999).

Pathological findings in two of the decedents were quite widespread and intriguing. Besides neuronal loss and gliosis, which were most predominant in the cerebellar cortex, substantia nigra, putamen, globus pallidus and dentate nucleus of the cerebellum, the most striking neuropathological features were widespread neuronal and glial tau pathology. Tangles were especially prominent in substantia nigra, putamen, globus pallidus and substantia innominata, subiculum, entorhinal cortex and the dentate nucleus. Interestingly, the severity of neuronal loss did not correlate with the amount of tau immunoreactivity. Cortical neuronal loss was mild, but there was moderate tau deposition in both neurons and glia. In contrast, cerebellar neuronal tau deposits were not observed in the cortex, although there was severe cortical neuronal loss. This finding has also been observed in other tauopathies, possibly because the cerebellum has a lower

endogenous tau content than do other brain regions (Bu *et al.*, 2002).

The two patients described here showed neuropathological changes reminiscent of those characterizing corticobasal degeneration (Dickson *et al.*, 2002). Similar to corticobasal degeneration, they showed severe neuronal loss of globus pallidus as well as of the substantia nigra, and moderate neuronal loss in the frontal and occipital cortices and subiculum and thalamic nuclei. These changes were associated with abundant neuronal and glial tau pathology, including coiled bodies and astrocytic plaques that are the characteristic features of corticobasal degeneration. Glial tau-positive inclusions resembling coiled bodies have been described in the white matter of patients with fronto-temporal lobar dementia (Kovacs *et al.*, 2008); however, this globular type of glial inclusion was not seen in our two cases.

In contrast to the characteristic findings in corticobasal degeneration, ballooned neurons that are a key feature of corticobasal degeneration were not identified in cerebral cortex or hippocampus for any of the subjects described here. Furthermore, the neuronal loss was most pronounced in hippocampal CA4 and subiculum as opposed to CA2 and CA3 as in corticobasal degeneration. Another distinct difference was the severe degeneration of cerebellar Purkinje cells and dentate nuclear neurons not usually seen in corticobasal degeneration (Brown *et al.*, 1996; Ikeda, 1997; Mori and Oda, 1997; Armstrong *et al.*, 2000; Dickson *et al.*, 2002).

Corticobasal degeneration is known to demonstrate both clinical and pathological variability, but is clinically distinct from the clinical syndrome demonstrated by the family we report here. Corticobasal degeneration is a disorder of late middle age characterized by clumsiness that typically begins on the non-dominant side, bradykinesia, dystonia, reflex myoclonus, dysarthria, ideomotor apraxia and relatively late-onset dementia (Litvan *et al.*, 1998; Mahapatra *et al.*, 2004; Belfor *et al.*, 2006). Although rare, familial occurrences of corticobasal degeneration have been reported, some caused by mutations affecting the *GRN* (formerly *PGRN*, or progranulin) gene (Masellis *et al.*, 2006; Rademakers *et al.*, 2007; Spina *et al.*, 2007; Guerreiro *et al.*, 2008; Benussi *et al.*, 2009; Yu *et al.*, 2010), but most cases are sporadic (Spillantini *et al.*, 2000; Lang, 2003; Uchihara and Nakayama, 2006).

Tau phosphoproteins bind to microtubules and are thought to promote the assembly and stability of microtubules, thereby playing a pivotal role in maintaining axonal transport as well as axonal integrity (reviewed in Buee *et al.*, 2000; Lee *et al.*, 2001). In the adult human central nervous system, six tau isoforms are produced by alternative splicing (Goedert *et al.*, 1989). Alternative splicing of exons 2 and 3 results in the insertion of 0 (0N), 1 (1N) or 2 (2N) 29-amino acid long motifs near the amino terminus, whereas splicing of exon 10 results in the inclusion of either 3 (3R) or 4 (4R) microtubule-binding domains in the carboxy terminus. Splicing of exons 2, 3 and 10 is tightly regulated to maintain similar levels of 4R to 3R isoforms in the normal human brain (Goedert and Jakes, 1990). The distinct tauopathies, however, differ in their relative amounts of the six tau isoforms in insoluble tau deposits. For example, in Alzheimer's disease, both the 3R and 4R isoforms are abnormally phosphorylated, leading to aggregation of all six isoforms into paired helical filaments (Hong *et al.*, 1998). Inclusions in Pick disease contain predominantly 3R isoforms (Delacourte *et al.*, 1996), while the major pathological tau isoforms in progressive supranuclear palsy and corticobasal degeneration consist primarily of 4R (Arai *et al.*, 2001; Forman *et al.*, 2002; Zhukareva *et al.*, 2006). Based on the present pathology, progressive supranuclear palsy was considered in the differential diagnosis. Progressive supranuclear palsy is characterized by neuronal loss and the presence of tangles in globus pallidus, putamen, substantia nigra, dentate and olivary nuclei (Hauw *et al.*, 1990) as well as a preponderance of 4R tau isoforms (Sergeant *et al.*, 1999). However, progressive supranuclear palsy presents much later in life than does the syndrome described here, and severe degeneration of cerebellar Purkinje cells seen in the present cases is not usually seen in progressive supranuclear palsy.

Sarkosyl-insoluble tau extracted from brain tissue from the two family members contained a clear preponderance of 4R isoforms, which are also the predominant isoforms deposited in progressive supranuclear palsy and corticobasal degeneration (Forman *et al.*, 2002; Zhukareva *et al.*, 2006).

The morphological substrate(s) for mental retardation are diverse and may not have a common underlying basis. Of the mental retardation syndromes, the neuropathologically best-studied entities are Down's syndrome, fragile X mental retardation, Rett syndrome, MASA (mental retardation, aphasia, shuffling gait and adducted thumbs) syndrome and West's syndrome (also called Partington syndrome, Proud syndrome and X-linked lissencephaly). The most striking abnormalities in Down's syndrome are β-amyloid deposits and the extensive presence of neurofibrillary tangles similar to those seen in individuals with Alzheimer's disease (Glenner and Wong, 1984; Masters *et al.*, 1985; Wisniewski and Wrzolek, 1988) and may be caused by overexpression of the *APP* gene, which is located on chromosome 21 (Cataldo *et al.*, 2003). Other pathological correlates with mental retardation include widespread dysmyelination in Pelizaeus-Merzbacher disease (Seitelberger, 1970; Seitelberger *et al.*, 1996; Sima *et al.*, 2009), aqueductal stenosis and ventriculomegaly in MASA syndrome (Jouet *et al.*, 1994; Vits *et al.*, 1994), lissencephaly (Gleeson *et al.*, 1998; Pilz *et al.*, 1998), cortical heterotopias (Gleeson *et al.*, 1998), cerebellar pathology (Tentler *et al.*, 1999; Bergmann *et al.*, 2003; Huber, 2006) and other severe disturbances of cerebral development (Eksioglu *et al.*, 1996). More subtle abnormalities, such as disturbance in maturation of dendritic spines, may be the primary finding, as in Rett syndrome (Jellinger *et al.*, 1988; Armstrong, 2005) and in fragile X mental retardation (Hinton *et al.*, 1991; Wisniewski *et al.*, 1991). Many types of X-linked mental retardation, however, have either shown no identifiable neuropathology or have not been characterized pathologically.

We speculate that the clinical deterioration noted in affected members of the present family results from progressive neuro-degeneration that is, at least in part, caused by the tau deposition. Whether the tau deposition also is responsible for the childhood-onset severe mental retardation is at this time unclear, since we only have pathological material from two middle-aged affected males. However, since the tau deposition is so widespread and intense, we believe it is likely to have been long-standing in the affected individuals and have contributed to

the mental retardation phenotype. It is possible that other factors lead to mental retardation, and we cannot exclude the possibility that these unknown determinants trigger the tau deposition.

The present pathological observations of a family with a form of syndromic X-linked severe mental retardation, we believe, have not been previously demonstrated. The demarcation between syndromic and non-syndromic mental retardation is not precise, and previously regarded non-syndromic forms of mental retardation may have additional clinical findings that were not initially recognized or emphasized, such as the cerebellar hypoplasia seen in mutations of the oligophrenin 1 (*OPHN1*) gene (Philip *et al.*, 2003). The presence of seizures in most of the patients as well as relatively late-onset motor deterioration, reminiscent of that seen in patients with corticobasal degeneration, we believe, reflect the underlying pathology in this family, and constitute distinctive clinical findings that can help differentiate this syndrome from other forms of X-linked mental retardation.

Analysis of another in-frame deletion (del 255–256) of *SLC9A6* has shown that the mutant protein undergoes aberrant processing and degradation in both the proteosomal and lysosomal compartments (Roxrud *et al.*, 2009). While the yeast homolog of SLC9A6, Nhx1, has been shown to be important for both vesicular pH regulation and intracellular vesicular targeting, the del 255–256 mutant protein does not appear to perturb vesicular pH (Gilfillan *et al.*, 2008; Roxrud *et al.*, 2009), although depletion of both SLC9A6 (sodium/hydrogen exchanger 6) and SLC9A9 (sodium/hydrogen exchanger 9) does cause excessive acidification of early endosomes (Roxrud *et al.*, 2009). Therefore, perturbation of endosomal pH does not appear to be the cause of cellular pathology in *SLC9A6*-related mental retardation. However, a further study will be needed to clarify the molecular and cellular mechanisms of neuronal dysfunction and mental retardation, as well as the conformational and processing effects on SLC9A6 of the mutation found in the reported family.

The discovery that this family's syndrome results from an *SLC9A6* mutation demonstrates that a disturbance in a membrane transport protein can lead to tau aggregation. The del 255–256 mutant protein as well as wild-type SLC9A6 is transported by a dynein-dependent mechanism (Roxrud *et al.*, 2009). Other proteins related to SLC9A6 have been shown to interact with elements of the cytoskeleton and may be critical for proper intracellular vesicular trafficking (Orlowski and Grinstein, 2004). Together, these observations suggest that the deposition of tau may be mediated by the interaction with the mutant SLC9A6 protein. The clear preponderance of 4R tau isoforms in the sarkosyl-insoluble tau isolated from the patients examined here is intriguing, since these are also the predominant isoforms deposited in the neuropathologically similar progressive supranuclear palsy and corticobasal degeneration syndromes (Forman *et al.*, 2002; Zhukareva *et al.*, 2006). Progressive supranuclear palsy and corticobasal degeneration are disorders of unknown aetiology and most cases do not appear to have an obvious Mendelian basis.

We speculate that the gene defect in this family may either result in aberrant exon 10 splicing of *MAPT*, leading to the observed tau isoform expression pattern, or somehow selectively stabilize it, perhaps in the form of aggregates with the mutated SLC9A6 protein. Disturbance in splicing is strongly suggested as a mechanism in neurodegenerative disease by the recent discovery that TDP-43 (also called TARDBP), an RNA-binding protein implicated in exon skipping and transcriptional regulation (Buratti *et al.*, 2004; Mercado *et al.*, 2005), is a major component of ubiquitin-immunoreactive inclusions in sporadic amyotrophic lateral sclerosis, in which aberrant splicing has been demonstrated (Neumann *et al.*, 2006). TDP-43 inclusions are also described in amyotrophic lateral sclerosis with dementia, non-*SOD1*-associated familial amyotrophic lateral sclerosis and in fronto-temporal lobar degeneration with ubiquitin inclusions (Arai *et al.*, 2006; Cairns *et al.*, 2007; Neumann *et al.*, 2007; Tan *et al.*, 2007). The absence of TDP-43 inclusions in our cases suggests that a different mechanism underlies the generation of the tau isoform pattern in *SLC9A6*-related mental retardation. Myotonic dystrophy 1 is another disorder in which perturbation in splicing is implicated as a major mechanism in disease pathogenesis. Cerebral neurofibrillary degeneration and mental retardation occur in severe cases of myotonic dystrophy 1, and it is characterized by abnormal RNA splicing of numerous genes, including *MAPT*, although the precise mechanism(s) has not yet been identified (Maurage *et al.*, 2005; Leroy *et al.*, 2006; Wang *et al.*, 2007). Identification of a mutation in *SLC9A6* in the family presented in this report may provide important insights not only into the underlying pathogenic mechanisms leading to this novel mental retardation and autism syndrome, but also to that of tau-associated dementias, such as those important in the regulation and splicing of the *MAPT* gene and in the processing of the tau metabolism abnormality.

Acknowledgements

We thank colleagues for technical support and advice in the Centre for Neurodegenerative Disease Research. We thank the families of patients whose generosity made this research possible. V. M. Y. L. is the John H. Ware, Third Chair of Alzheimer's disease research; and J.Q.T. is the William Maul Measey-Truman G. Schnabel, Jr., Professor of Geriatric Medicine and Gerontology. J.Y.G. is grateful to Dr Rajini Rao for helpful discussions.

Funding

National Institutes of Health (AG-09215, AG-10124, AG-17586).

Supplementary material

Supplementary material is available at *Brain* online.

References

Arai T, Hasegawa M, Akiyama H, Ikeda K, Nonaka T, Mori H, et al. TDP-43 is a component of ubiquitin-positive tau-negative inclusions in frontotemporal lobar degeneration and amyotrophic lateral sclerosis. Biochem Biophys Res Commun 2006; 351: 602–11.

Arai T, Ikeda K, Akiyama H, Shikamoto Y, Tsuchiya K, Yagishita S, et al. Distinct isoforms of tau aggregated in neurons and glial cells in brains

of patients with Pick's disease, corticobasal degeneration and progressive supranuclear palsy. Acta Neuropathol 2001; 101: 167–73.
Armstrong DD. Neuropathology of Rett syndrome. J Child Neurol 2005; 20: 747–53.
Armstrong RA, Cairns NJ, Lantos PL. A quantitative study of the pathological lesions in the neocortex and hippocampus of twelve patients with corticobasal degeneration. Exp Neurol 2000; 163: 348–56.
Belfor N, Amici S, Boxer AL, Kramer JH, Gorno-Tempini ML, Rosen HJ, et al. Clinical and neuropsychological features of corticobasal degeneration. Mech Ageing Dev 2006; 127: 203–7.
Benussi L, Ghidoni R, Pegoiani E, Moretti DV, Zanetti O, Binetti G. Progranulin Leu271LeufsX10 is one of the most common FTLD and CBS associated mutations worldwide. Neurobiol Dis 2009; 33: 379–85.
Bergmann C, Zerres K, Senderek J, Rudnik-Schoneborn S, Eggermann T, Hausler M, et al. Oligophrenin 1 (OPHN1) gene mutation causes syndromic X-linked mental retardation with epilepsy, rostral ventricular enlargement and cerebellar hypoplasia. Brain 2003; 126: 1537–44.
Brown J, Lantos PL, Roques P, Fidani L, Rossor MN. Familial dementia with swollen achromatic neurons and corticobasal inclusion bodies: a clinical and pathological study. J Neurol Sci 1996; 135: 21–30.
Bu B, Klunemann H, Suzuki K, Li J, Bird T, Jin LW, et al. Niemann-Pick disease type C yields possible clue for why cerebellar neurons do not form neurofibrillary tangles. Neurobiol Dis 2002; 11: 285–97.
Buee L, Bussiere T, Buee-Scherrer V, Delacourte A, Hof PR. Tau protein isoforms, phosphorylation and role in neurodegenerative disorders. Brain Res Brain Res Rev 2000; 33: 95–130.
Buratti E, Brindisi A, Pagani F, Baralle FE. Nuclear factor TDP-43 binds to the polymorphic TG repeats in CFTR intron 8 and causes skipping of exon 9: a functional link with disease penetrance. Am J Hum Genet 2004; 74: 1322–5.
Bushby KM, Cole T, Matthews JN, Goodship JA. Centiles for adult head circumference. Arch Dis Child 1992; 67: 1286–7.
Cairns NJ, Neumann M, Bigio EH, Holm IE, Troost D, Hatanpaa KJ, et al. TDP-43 in familial and sporadic frontotemporal lobar degeneration with ubiquitin inclusions. Am J Pathol 2007; 171: 227–40.
Cataldo AM, Petanceska S, Peterhoff CM, Terio NB, Epstein CJ, Villar A, et al. App gene dosage modulates endosomal abnormalities of Alzheimer's disease in a segmental trisomy 16 mouse model of down syndrome. J Neurosci 2003; 23: 6788–92.
Christianson AL, Stevenson RE, van der Meyden CH, Pelser J, Theron FW, van Rensburg PL, et al. X linked severe mental retardation, craniofacial dysmorphology, epilepsy, ophthalmoplegia, and cerebellar atrophy in a large South African kindred is localised to Xq24-q27. J Med Genet 1999; 36: 759–66.
Cottingham RW Jr, Idury RM, Schaffer AA. Faster sequential genetic linkage computations. Am J Hum Genet 1993; 53: 252–63.
Delacourte A, Robitaille Y, Sergeant N, Buee L, Hof PR, Wattez A, et al. Specific pathological Tau protein variants characterize Pick's disease. J Neuropathol Exp Neurol 1996; 55: 159–68.
Dickson DW, Bergeron C, Chin SS, Duyckaerts C, Horoupian D, Ikeda K, et al. Office of Rare Diseases neuropathologic criteria for corticobasal degeneration. J Neuropathol Exp Neurol 2002; 61: 935–46.
Eksioglu YZ, Scheffer IE, Cardenas P, Knoll J, DiMario F, Ramsby G, et al. Periventricular heterotopia: an X-linked dominant epilepsy locus causing aberrant cerebral cortical development. Neuron 1996; 16: 77–87.
Forman MS, Schmidt ML, Kasturi S, Perl DP, Lee VM, Trojanowski JQ. Tau and alpha-synuclein pathology in amygdala of Parkinsonism-dementia complex patients of Guam. Am J Pathol 2002; 160: 1725–31.
Forman MS, Zhukareva V, Bergeron C, Chin SS, Grossman M, Clark C, et al. Signature tau neuropathology in gray and white matter of corticobasal degeneration. Am J Pathol 2002; 160: 2045–53.
Giasson BI, Jakes R, Goedert M, Duda JE, Leight S, Trojanowski JQ, et al. A panel of epitope-specific antibodies detects protein domains distributed throughout human alpha-synuclein in Lewy bodies of Parkinson's disease. J Neurosci Res 2000; 59: 528–33.
Gilfillan GD, Selmer KK, Roxrud I, Smith R, Kyllerman M, Eiklid K, et al. SLC9A6 mutations cause X-linked mental retardation, microcephaly, epilepsy, and ataxia, a phenotype mimicking Angelman syndrome. Am J Hum Genet 2008; 82: 1003–10.
Gleeson JG, Allen KM, Fox JW, Lamperti ED, Berkovic S, Scheffer I, et al. Doublecortin, a brain-specific gene mutated in human X-linked lissencephaly and double cortex syndrome, encodes a putative signaling protein. Cell 1998; 92: 63–72.
Glenner GG, Wong CW. Alzheimer's disease and Down's syndrome: sharing of a unique cerebrovascular amyloid fibril protein. Biochem Biophys Res Commun 1984; 122: 1131–5.
Goedert M, Jakes R. Expression of separate isoforms of human tau protein: correlation with the tau pattern in brain and effects on tubulin polymerization. Embo J 1990; 9: 4225–30.
Goedert M, Jakes R, Crowther RA, Six J, Lubke U, Vandermeeren M, et al. The abnormal phosphorylation of tau protein at Ser-202 in Alzheimer disease recapitulates phosphorylation during development. Proc Natl Acad Sci USA 1993; 90: 5066–70.
Goedert M, Jakes R, Vanmechelen E. Monoclonal antibody AT8 recognises tau protein phosphorylated at both serine 202 and threonine 205. Neurosci Lett 1995; 189: 167–9.
Goedert M, Spillantini MG, Jakes R, Rutherford D, Crowther RA. Multiple isoforms of human microtubule-associated protein tau: sequences and localization in neurofibrillary tangles of Alzheimer's disease. Neuron 1989; 3: 519–26.
Greenberg SG, Davies P. A preparation of Alzheimer paired helical filaments that displays distinct tau proteins by polyacrylamide gel electrophoresis. Proc Natl Acad Sci USA 1990; 87: 5827–31.
Guerreiro RJ, Santana I, Bras JM, Revesz T, Rebelo O, Ribeiro MH, et al. Novel progranulin mutation: screening for PGRN mutations in a Portuguese series of FTD/CBS cases. Mov Disord 2008; 23: 1269–73.
Hauw JJ, Verny M, Delaere P, Cervera P, He Y, Duyckaerts C. Constant neurofibrillary changes in the neocortex in progressive supranuclear palsy. Basic differences with Alzheimer's disease and aging. Neurosci Lett 1990; 119: 182–6.
Hinton VJ, Brown WT, Wisniewski K, Rudelli RD. Analysis of neocortex in three males with the fragile X syndrome. Am J Med Genet 1991; 41: 289–94.
Hong M, Zhukareva V, Vogelsberg-Ragaglia V, Wszolek Z, Reed L, Miller BI, et al. Mutation-specific functional impairments in distinct tau isoforms of hereditary FTDP-17. Science 1998; 282: 1914–7.
Huber KM. The fragile X-cerebellum connection. Trends Neurosci 2006; 29: 183–5.
Ikeda K. Basic pathology of corticobasal degeneration. Neuropathology 1997; 17: 127–33.
Jellinger K, Armstrong D, Zoghbi HY, Percy AK. Neuropathology of Rett syndrome. Acta Neuropathol 1988; 76: 142–58.
Jouet M, Rosenthal A, Armstrong G, MacFarlane J, Stevenson R, Paterson J, et al. X-linked spastic paraplegia (SPG1), MASA syndrome and X-linked hydrocephalus result from mutations in the L1 gene. Nat Genet 1994; 7: 402–7.
Kosik KS, Orecchio LD, Binder L, Trojanowski JQ, Lee VM, Lee G. Epitopes that span the tau molecule are shared with paired helical filaments. Neuron 1988; 1: 817–25.
Kovacs GG, Majtenyi K, Spina S, Murrell JR, Gelpi E, Hoftberger R, et al. White matter tauopathy with globular glial inclusions: a distinct sporadic frontotemporal lobar degeneration. J Neuropathol Exp Neurol 2008; 67: 963–75.
Lang AE. Corticobasal degeneration: selected developments. Mov Disord 2003; 18(Suppl 6): S51–6.
Lathrop GM, Lalouel JM, Julier C, Ott J. Strategies for multilocus linkage analysis in humans. Proc Natl Acad Sci USA 1984; 81: 3443–6.
Lee VM, Balin BJ, Otvos L Jr, Trojanowski JQ. A68: a major subunit of paired helical filaments and derivatized forms of normal Tau. Science 1991; 251: 675–8.
Lee VM, Goedert M, Trojanowski JQ. Neurodegenerative tauopathies. Annu Rev Neurosci 2001; 24: 1121–59.
Leroy O, Wang J, Maurage CA, Parent M, Cooper T, Buee L, et al. Brain-specific change in alternative splicing of Tau exon 6 in myotonic dystrophy type 1. Biochim Biophys Acta 2006; 1762: 460–7.

Litvan II, Jankovic J, Goetz CG, Wenning GK, Sastry N, Jellinger K, et al. Accuracy of the clinical diagnosis of postencephalitic parkinsonism: a clinicopathologic study. Eur J Neurol 1998; 5: 451–7.

Mahapatra RK, Edwards MJ, Schott JM, Bhatia KP. Corticobasal degeneration. Lancet Neurol 2004; 3: 736–43.

Masellis M, Momeni P, Meschino W, Heffner R Jr, Elder J, Sato C, et al. Novel splicing mutation in the progranulin gene causing familial corticobasal syndrome. Brain 2006; 129: 3115–23.

Masters CL, Simms G, Weinman NA, Multhaup G, McDonald BL, Beyreuther K. Amyloid plaque core protein in Alzheimer disease and Down syndrome. Proc Natl Acad Sci U S A 1985; 82: 4245–9.

Maurage CA, Udd B, Ruchoux MM, Vermersch P, Kalimo H, Krahe R, et al. Similar brain tau pathology in DM2/PROMM and DM1/Steinert disease. Neurology 2005; 65: 1636–8.

Mawal-Dewan M, Schmidt ML, Balin B, Perl DP, Lee VM, Trojanowski JQ. Identification of phosphorylation sites in PHF-TAU from patients with Guam amyotrophic lateral sclerosis/parkinsonism-dementia complex. J Neuropathol Exp Neurol 1996; 55: 1051–9.

Mercado PA, Ayala YM, Romano M, Buratti E, Baralle FE. Depletion of TDP 43 overrides the need for exonic and intronic splicing enhancers in the human apoA-II gene. Nucleic Acids Res 2005; 33: 6000–10.

Mercken M, Vandermeeren M, Lubke U, Six J, Boons J, Van de Voorde A, et al. Monoclonal antibodies with selective specificity for Alzheimer Tau are directed against phosphatase-sensitive epitopes. Acta Neuropathol 1992; 84: 265–72.

Mori H, Oda M. Ballooned neurons in corticobasal degeneration and progressive supranuclear palsy. Neuropathlogy 1997; 17: 148–52.

Neumann M, Mackenzie IR, Cairns NJ, Boyer PJ, Markesbery WR, Smith CD, et al. TDP-43 in the ubiquitin pathology of frontotemporal dementia with VCP gene mutations. J Neuropathol Exp Neurol 2007; 66: 152–7.

Neumann M, Sampathu DM, Kwong LK, Truax AC, Micsenyi MC, Chou TT, et al. Ubiquitinated TDP-43 in frontotemporal lobar degeneration and amyotrophic lateral sclerosis. Science 2006; 314: 130–3.

Orlowski J, Grinstein S. Diversity of the mammalian sodium/proton exchanger SLC9 gene family. Pflugers Arch 2004; 447: 549–65.

Philip N, Chabrol B, Lossi AM, Cardoso C, Guerrini R, Dobyns WB, et al. Mutations in the oligophrenin-1 gene (OPHN1) cause X linked congenital cerebellar hypoplasia. J Med Genet 2003; 40: 441–6.

Pilz DT, Matsumoto N, Minnerath S, Mills P, Gleeson JG, Allen KM, et al. LIS1 and XLIS (DCX) mutations cause most classical lissencephaly, but different patterns of malformation. Hum Mol Genet 1998; 7: 2029–37.

Rademakers R, Baker M, Gass J, Adamson J, Huey ED, Momeni P, et al. Phenotypic variability associated with progranulin haploinsufficiency in patients with the common 1477C–>T (Arg493X) mutation: an international initiative. Lancet Neurol 2007; 6: 857–68.

Ropers HH. X-linked mental retardation: many genes for a complex disorder. Curr Opin Genet Dev 2006; 16: 260–9.

Roxrud I, Raiborg C, Gilfillan GD, Stromme P, Stenmark H. Dual degradation mechanisms ensure disposal of NHE6 mutant protein associated with neurological disease. Exp Cell Res 2009; 315: 3014–27.

Schmidt ML, Carden MJ, Lee VM, Trojanowski JQ. Phosphate dependent and independent neurofilament epitopes in the axonal swellings of patients with motor neuron disease and controls. Lab Invest 1987; 56: 282–94.

Schopler E, Reichler RJ, DeVellis RF, Daly K. Toward objective classification of childhood autism: Childhood Autism Rating Scale (CARS). J Autism Dev Disord 1980; 10: 91–103.

Seitelberger F. Pelizaeus-Merzbacher disease. In: Vinken PJ, Bruyn GW, editors. Handbook of clinical neurology. Amsterdam: North Holland Publishing Co; 1970. p. 150–220.

Seitelberger F, Urbanits S, Nave K-A. Pelizaeus-Merzbacher disease. In: Moser HW, editor. Neurodystrophies and neurolipidoses. Amsterdam: Elsevier Science; 1996. p. 559–79.

Sergeant N, Wattez A, Delacourte A. Neurofibrillary degeneration in progressive supranuclear palsy and corticobasal degeneration: tau pathologies with exclusively "exon 10" isoforms. J Neurochem 1999; 72: 1243–9.

Seubert P, Mawal-Dewan M, Barbour R, Jakes R, Goedert M, Johnson GV, et al. Detection of phosphorylated Ser262 in fetal tau, adult tau, and paired helical filament tau. J Biol Chem 1995; 270: 18917–22.

Sima AA, Defendini R, Keohane C, D'Amato C, Foster NL, Parchi P, et al. The neuropathology of chromosome 17-linked dementia. Ann Neurol 1996; 39: 734–43.

Sima AA, Pierson CR, Woltjer RL, Hobson GM, Golden JA, Kupsky WJ, et al. Neuronal loss in Pelizaeus-Merzbacher disease differs in various mutations of the proteolipid protein 1. Acta Neuropathol 2009; 118: 531–9.

Spillantini MG, Yoshida H, Rizzini C, Lantos PL, Khan N, Rossor MN, et al. A novel tau mutation (N296N) in familial dementia with swollen achromatic neurons and corticobasal inclusion bodies. Ann Neurol 2000; 48: 939–43.

Spina S, Murrell JR, Huey ED, Wassermann EM, Pietrini P, Grafman J, et al. Corticobasal syndrome associated with the A9D Progranulin mutation. J Neuropathol Exp Neurol 2007; 66: 892–900.

Tan Z, Sun X, Hou FS, Oh HW, Hilgenberg LG, Hol EM, et al. Mutant ubiquitin found in Alzheimer's disease causes neuritic beading of mitochondria in association with neuronal degeneration. Cell Death Differ 2007; 14: 1721–32.

Tentler D, Gustavsson P, Leisti J, Schueler M, Chelly J, Timonen E, et al. Deletion including the oligophrenin-1 gene associated with enlarged cerebral ventricles, cerebellar hypoplasia, seizures and ataxia. Eur J Hum Genet 1999; 7: 541–8.

Uchihara T, Nakayama H. Familial tauopathy mimicking corticobasal degeneration an autopsy study on three siblings. J Neurol Sci 2006.

Vits L, Van Camp G, Coucke P, Fransen E, De Boulle K, Reyniers E, et al. MASA syndrome is due to mutations in the neural cell adhesion gene L1CAM. Nat Genet 1994; 7: 408–13.

Wang J, Tse SW, Andreadis A. Tau exon 6 is regulated by an intricate interplay of trans factors and cis elements, including multiple branch points. J Neurochem 2007; 100: 437–45.

Winton MJ, Joyce S, Zhukareva V, Practico D, Perl DP, Galasko D, et al. Characterization of tau pathologies in gray and white matter of Guam parkinsonism-dementia complex. Acta Neuropathol 2006; 111: 401–12.

Wisniewski HM, Wrzolek M. Pathogenesis of amyloid formation in Alzheimer's disease, Down's syndrome and scrapie. Ciba Found Symp 1988; 135: 224–38.

Wisniewski KE, Segan SM, Miezejeski CM, Sersen EA, Rudelli RD. The Fra(X) syndrome: neurological, electrophysiological, and neuropathological abnormalities. Am J Med Genet 1991; 38: 476–80.

Yu CE, Bird TD, Bekris LM, Montine TJ, Leverenz JB, Steinbart E, et al. The spectrum of mutations in progranulin: a collaborative study screening 545 cases of neurodegeneration. Arch Neurol 2010; 67: 161–70.

Zhukareva V, Joyce S, Schuck T, Van Deerlin V, Hurtig H, Albin R, et al. Unexpected abundance of pathological tau in progressive supranuclear palsy white matter. Ann Neurol 2006; 60: 335–45.

Zhukareva V, Mann D, Pickering-Brown S, Uryu K, Shuck T, Shah K, et al. Sporadic Pick's disease: a tauopathy characterized by a spectrum of pathological tau isoforms in gray and white matter. Ann Neurol 2002; 51: 730–9.

Zhukareva V, Shah K, Uryu K, Braak H, Del Tredici K, Sundarraj S, et al. Biochemical analysis of tau proteins in argyrophilic grain disease, Alzheimer's disease, and Pick's disease: a comparative study. Am J Pathol 2002; 161: 1135–41.